Structural Variations in the $[Mo_4As_6O_{20}(OH)_2]^{4-}$ Core: Influence of Cation Structure on Mo···Mo Distances

M. Ishaque Khan, Qin Chen, and Jon Zubieta*

Department of Chemistry, Syracuse University,
Syracuse, New York 13244

Received June 11, 1993

While the W/As/O and V/As/O systems have been shown to give a variety of structurally unusual heteropolyanion clusters,[1-16] the Mo/As/O polyanions remain relatively undeveloped. Clusters containing As(V) are represented by the fully-oxidized and mixed valence Keggin cores $[Mo_{12}AsO_{40}]^{3-}$ and $[H_nMo^{V}{}_nMo^{VI}{}_{12-n}AsO_{40}]^{3-}$ ($n = 2$ and 4),[17] respectively, and the Dawson polyanion $[Mo_{18}As_2O_{62}]^{6-}$.[18] Incorporation of As(III) sites has been reported for the Mo(V)/Mo(VI) mixed-valence clusters $[H_6As_{10}Mo_{24}O_{90}]^{-}$ [19] and $[H_4As_3Mo_{12}O_{40}]^{-}$ [20] and for the $(As_3O_7)^{5-}$-containing Mo(VI) clusters $[Mo_3As_3O_{15}]^{3-}$ and $[Mo_6CoAs_6O_{30}]^{4-}$.[21] In the course of our investigations of the hydrothermal reactions of molybdenum oxides with arsenic-containing species under reducing conditions, an unusual example of an arsenic rich Mo/As/O cluster, $Na_4[Mo_4As_6O_{20}(OH)_2]\cdot 9H_2O$ (**1**) was prepared.[22]

In common with many of the hydrothermal syntheses, it was subsequently discovered that minor modifications in reaction conditions yielded a structurally distinct composition, $Na_4[Mo_4As_6O_{20}(OH)_2]\cdot 10H_2O$ (**2**). While the structures of the anions of **1** and **2** are identical in most details, the Mo–Mo distances within the Mo(V)–Mo(V) binuclear units of the core are significantly different, 2.770(2) Å in **1** and 2.613(1) Å in **2**. This bond length difference is related to the different cation environments displayed by **1** and **2**.

Experimental Section

Preparation of $Na_4[Mo_4As_6O_{20}(OH)_2]\cdot 9H_2O$ (1). A mixture of $Na_2MoO_4\cdot 2H_2O$, MoO_3, Mo (−325 mesh, Cerac), $H_5As_3O_{10}$, NaCl, Et_4NOH, and H_2O in the mole ratio 6:6:6:3:10:10:166 was heated in a 23-mL Teflon-lined Parr acid digestion bomb for 110 h at 180 °C and autogenous pressure. The dark brown solution which was produced was filtered to remove an amorphous tan solid. The filtrate was allowed to stand at room temperature for 4 days, whereupon red crystals were collected in 50% yield. As the crystals become opaque upon drying, they were stored in the presence of a small amount of the mother liquor. Anal. Calcd for $H_{20}O_{31}Na_4As_6Mo_4$: H, 1.39; Mo, 26.6. Found: H, 1.25; Mo, 26.3. IR (KBr pellet, cm^{-1}): 1261 (vs), 1092 (vs), 1021 (s), 947 (s), 799 (vs), 717 (m), 622 (m), 506 (m).

Preparation of $Na_4[Mo_4As_6O_{20}(OH)_2]\cdot 10H_2O$ (2). A mixture of $Na_2MoO_4\cdot 2H_2O$, MoO_3, Mo (−325 mesh), $C_6H_5AsO_3H_2$, NaCl, Et_4NOH, and H_2O in the mole ratio 6:6:6:10:10:10:111 was heated in a Teflon-lined Parr acid digestion bomb for 120 h at 180 °C. The resultant red-brown solution was allowed to stand at room temperature for 2 weeks whereupon the solution color was discharged and red crystals of **2** were isolated in 40% yield. The crystals of **2** rapidly became opaque when removed from the mother liquor. Anal. Calcd for $H_{22}O_{32}Na_4Mo_4As_6$: H, 1.50; Mo, 26.2. Found: H, 1.52; Mo, 26.3. IR (KBr pellet, cm^{-1}): 1260 (vs), 1090 (s), 1020 (s), 947 (s), 927 (sh), 798 (vs), 720 (s), 623 (m), 506 (m).

X-ray Crystal Structure Determination. Crystals of approximate dimensions 0.22 × 0.37 × 0.19 mm and 0.25 × 0.31 × 0.33 mm were used in the structure determinations of **1** and **2**, respectively. Since crystals of both **1** and **2** became opaque upon removal from the mother liquor with concomitant loss of diffraction intensity, both crystals were mounted in capillary tubes in the presence of the mother liquor. Unit cells constants were determined by least-squares fits to the setting parameters of 25 reflections with $2\theta \geq 22°$, measured on a Rigaku AFC5S diffractometer. Crystallographic details are presented in Table I. The structures were solved and refined using the SHELXTL program package. All non-hydrogen atoms were refined anisotropically, while hydrogen atoms were placed at calculated positions with fixed isotropic thermal parameters. Atomic positional parameters and isotropic temperature factors for **1** and **2** are presented in Tables II and III, respectively. Selected bond lengths and angles are summarized in Table IV.

Results and Discussion

The hydrothermal reaction of $Na_2MoO_4\cdot 2H_2O$, MoO_3, Mo, $H_5As_3O_{10}$, Et_4NOH, and H_2O for 110 h at 180 °C and autogenous pressure yields, after appropriate workup, red crystals of $Na_4[Mo_4As_6O_{20}(OH)_2]\cdot 9H_2O$ (**1**). While Et_4NOH does not appear in the product in any form, it is absolutely essential to the isolation of **1** as a monophasic crystalline material. While the role of such organic components in hydrothermal syntheses is not clear, the influence of such species as templates or in the adjustment of reaction pH have been noted.[23] Replacement of $H_5As_3O_{10}$ by phenylarsonic acid provides an analogous species of composition $Na_4[Mo_4As_6O_{20}(OH)_2]\cdot 10H_2O$ (**2**). Under the reducing conditions of the hydrothermal reaction, $C_6H_5AsO_3H_2$ apparently undergoes reduction and hydrolysis/condensation to provide the unusual $(HAs_3O_7)^-$ units associated with the structure. The isolation of **2** rather than **1** does not appear to reflect simple stoichiometry changes, such as the slightly higher As concentration in the optimized preparation of **2** relative to that employed for **1**. Variations in stoichiometry using $H_5As_3O_{10}$ as the arsenic source invariably resulted in formation of **1**, albeit in lower yields than for the optimized preparation which we report. On the other hand, we have observed that organoarsonates readily undergo a variety of condensation-type reactions to yield oligomeric arsenic oxides, such as $[R_6As_6O_8]^{4-}$ and $[As_nO_{2n+1}]^{2-}$. The infrared spectra of **1** and **2** are nearly identical with prominent features at 1092 and 1021 cm^{-1} associated with ν(As—O) and at 947 and 799 cm^{-1} characteristic of $\nu(Mo{=}O_t)$ and ν(Mo—O—Mo), respectively. However, since the powder diffraction patterns for **1** and **2** confirmed that the structures were not isomorphous, the X-ray crystallographic studies of both species were undertaken.

---

(1) Robert, F.; Leyrie, M.; Hervé, G.; Teze, A.; Jeannin, Y. *Inorg. Chem.* **1980**, *19*, 1746.
(2) Martin-Frère, J.; Jeannin, Y.; Robert, F.; Vaisserman, J. *Inorg. Chem.* **1991**, *30*, 3635.
(3) Hervé, G. *Inorg. Synth.* **1990**, *27*, 118.
(4) Leyrie, M.; Martin-Frère, J.; Hervé, G. *C. R. Acad. Sci., Ser. C* **1974**, *279*, 895.
(5) Tourné, C.; Revel, A.; Tourné, G.; Vendrell, M. *C. R. Acad. Sci., Ser. C* **1973**, *277*, 643.
(6) Martin-Frère, J.; Jeannin, Y. *J. Am. Chem. Soc.* **1981**, *103*, 1664.
(7) Jeannin, Y. *Inorg. Chim. Acta* **1992**, *198-200*, 319.
(8) Müller, A.; Döring, J. *Z. Anorg. Allg. Chem.* **1991**, *595*, 251.
(9) Barra, A.-L.; Gatteschi, D.; Tsukerblatt, B. S.; Döring, J.; Müller, A.; Brunel, L.-C. *Inorg. Chem.* **1992**, *31*, 5132.
(10) Müller, A.; Penk, M.; Döring, J. *Inorg. Chem.* **1991**, *30*, 4935.
(11) Müller, A.; Döring, J.; Khan, M. I.; Wittenbun, V. *Angew. Chem., Int. Ed. Engl.* **1991**, *30*, 210.
(12) Müller, A.; Döring, J.; Bögge, H. *J. Chem. Soc., Chem. Commun.* **1991**, 273.
(13) Pope, M. T.; Müller, A. *Angew. Chem., Int. Ed. Engl.* **1991**, *30*, 34.
(14) Müller, A.; Döring, J. *Angew. Chem., Int. Ed. Engl.* **1988**, *27*, 1721.
(15) Huan, G.; Greaney, M. A.; Jacobson, A. J. *J. Chem. Soc., Chem. Commun.* **1991**, 260.
(16) Khan, M. I.; Chen, Q.; Zubieta, J.; Goshorn, D.; Haushalter, R. C. *Inorg. Chem. Acta* **1992**, *191*, 97.
(17) Müller, A.; Krickemeyer, E.; Penk, J.; Wittenben, V.; Döring, J. *Angew. Chem., Int. Ed. Eng.* **1990**, *29*, 88.
(18) Souchay, P.; Contant, R.; Fruchart, J.-M. *C. R. Acad. Sci. Paris* **1967**, *264*, 976.
(19) Müller, A.; Krickemeyer, E.; Penk, M.; Wittenben, V.; Döring, J. *Angew. Chem., Int. Ed. Engl.* **1990**, *29*, 88.
(20) Khan, M. I.; Chen, Q.; Zubieta, J. *Inorg. Chem.*, in press.
(21) Martin-Frère, J.; Jeannin, Y.; Robert, F.; Vaissermann, J. *Inorg. Chem.* **1991**, *30*, 3635.
(22) Khan, M. I.; Chen, Q.; Zubieta, J. *J. Chem. Soc., Chem. Commun.* **1993**, 356.
(23) Haushalter, R. C.; Mundi, L. A. *Chem. Mater.* **1992**, *4*, 31.

0020-1669/93/1332-5408$04.00/0

Table I. Crystallographic Data for $Na_4[Mo_4As_6O_{20}(OH)_2]\cdot 9H_2O$ (**1**) and $Na_4[Mo_4As_6O_{20}(OH)_2]\cdot 10H_2O$ (**2**)

	1	**2**
fw	1441.5	1459.6
space group	$C2/c$	$P\bar{1}$
a, Å	16.858(3)	9.182(2)
b, Å	8.488(2)	10.550(2)
c, Å	21.753(4)	8.889(2)
α, deg		101.54(1)
β, deg	108.12(3)	99.84(2)
δ, deg		109.53(1)
V, Å^3	2958.3(15)	768.3(4)
Z	4	1
D_{calc}, g cm^{-3}	3.236	3.106
λ(Mo Kα), Å	0.710 73	0.710 73
μ, cm^{-1}	84.9	81.8
no. of obsd rflns, $I_o \geq 3\sigma(I_o)$	2456	2365
R^a	0.0751	0.0506
$R_w{}^b$	0.0878	0.0590

[a] $R = \sum||F_o| - |F_c||/\sum|F_o|$. [b] $R_w = [\sum w(|F_o| - |F_c|)^2/\sum w|F_o|^2]^{1/2}$.

Table II. Atomic Coordinates ($\times 10^4$) and Equivalent Isotropic Displacement Coefficients (Å^2 $\times$ 10^3) for **1**

	x	y	z	U(eq)^a
Mo(1)	466(1)	1267(2)	4670(1)	13(1)
Mo(2)	−852(1)	−235(2)	3773(1)	14(1)
As(1)	−1848(1)	−3242(2)	2850(1)	21(1)
As(2)	−1069(1)	−4264(2)	4342(1)	17(1)
As(3)	−2537(1)	−1666(2)	4155(1)	17(1)
Na(1)	−429(5)	3805(8)	3178(4)	30(3)
Na(2)	2074(5)	−831(9)	4446(4)	40(3)
O(1)	1780(7)	988(12)	5074(5)	15(2)
O(2)	358(7)	3056(12)	4301(5)	16(2)
O(3)	435(7)	−323(13)	4054(5)	18(2)
O(4)	−713(7)	735(12)	4589(5)	14(2)
O(5)	−1197(8)	1333(14)	3266(6)	22(2)
O(6)	−981(7)	−1898(14)	3083(6)	22(2)
O(7)	−605(7)	−2348(12)	4455(5)	14(2)
O(8)	−2105(7)	−876(13)	3632(5)	20(2)
O(9)	−1512(8)	−4396(14)	2343(6)	26(3)
O(10)	−1307(8)	−4629(14)	3515(6)	24(3)
O(11)	−2160(8)	−3690(15)	4207(6)	27(3)
O(12)	1496(11)	−3198(20)	4715(9)	54(4)
O(13)	1143(18)	−231(32)	3084(14)	113(9)
O(14)	508(10)	6077(18)	3365(7)	41(4)
O(15)	2650(18)	−2360(35)	3880(14)	116(9)
O(16)	0	7681(32)	7500	60(7)

[a] Equivalent isotropic U defined as one-third of the trace of the orthogonalized U_{ij} tensor.

The structure of the molecular anion common to **1** and **2**, shown in Figure 1, consists of the tetranuclear $\{Mo_4O_{16}\}$ core[24] in which six terminal and two doubly bridging oxygen atoms have been replaced by eight oxygen donors from the two linear triarsenate(III) groups $(HAs_3O_7)^{4-}$. the $\{Mo_4O_{16}\}^{12-}$ core contains two {Mo(V)–Mo(V)} binuclear units, which are common structural motifs in molybdenum chemistry, characteristically exhibiting Mo–O distances in the range 1.6–2.2 Å and Mo–Mo distances in the range 2.5–2.7 Å.[25,26] Several structures containing two {Mo(V)–Mo(V)} binuclear units in a compact array with Mo centers occupying the vertices of a rhomb[27] or of a distorted tetrahedron[23] have been described. The anions of **1** and **2** exhibit $\{Mo_4O_{16}\}^{12-}$ core structures in which the Mo(V) centers are present in the rhomboid arrangement, with the oxygen atoms defining a cubic closest-packed array in which the Mo centers occupy octahedral holes.

Table III. Atomic Coordinates ($\times 10^4$) and Equivalent Isotropic Displacement Coefficients (Å^2 $\times$ 10^3) for **2**

	x	y	z	U(eq)^a
Mo(1)	4658(1)	10832(1)	1683(1)	10(1)
Mo(2)	2835(1)	8169(1)	749(1)	10(1)
As(1)	−262(1)	5430(1)	−1648(1)	12(1)
As(2)	1881(1)	6762(1)	−3792(1)	11(1)
As(3)	4126(1)	5810(1)	−1473(1)	12(1)
Na(1)	1982(6)	10113(5)	−1995(6)	20(2)
Na(2)	−2352(7)	6461(5)	−4389(6)	26(2)
O(1)	4383(10)	12606(8)	1422(10)	15(2)
O(2)	4916(10)	11088(9)	3674(10)	17(2)
O(3)	2392(9)	9876(8)	658(9)	13(2)
O(4)	5120(9)	9160(8)	853(9)	10(2)
O(5)	2782(10)	7965(9)	2569(10)	17(2)
O(6)	485(9)	7137(8)	−351(9)	11(2)
O(7)	2871(9)	8124(8)	−1977(9)	11(2)
O(8)	3106(9)	6324(8)	−138(9)	13(2)
O(9)	−2322(10)	5236(9)	−2078(10)	20(2)
O(10)	−24(9)	5980(8)	−3411(9)	13(2)
O(11)	2724(10)	5539(9)	−3327(10)	15(2)
O(12)	2111(12)	9871(11)	−4665(12)	32(2)
O(13)	1815(10)	12276(9)	−951(10)	21(2)
O(14)	−728(10)	8672(9)	−2216(10)	19(2)
O(15)	−1034(12)	7909(11)	−5833(12)	33(2)
O(16)	−4701(14)	6591(12)	−5631(14)	45(3)

[a] Equivalent isotropic U defined as one-third of the trace of the orthogonalized U_{ij} tensor.

The central tetramolybdenum core is sandwiched by two $(HAs_3O_7)^-$ units, each of which is constructed from a chain of three corner-sharing $\{AsO_3\}$ pyramids. The $\{Mo_4O_{16}\}$ core shares four oxygen atoms with each trinuclear As(III) chain. Each chain contains two oxygens which bridge As(III) centers, four oxygens which bridge As(III) and Mo(V) sites in either doubly or triply bridging modes, and a pendant and protonated oxygen associated with a terminal As site of the chain. The pyramidal geometries of the As(III) sites are consistent with the presence of the stereochemically active lone pair of electrons, a structural feature similar to that observed for $[Mo_3As_3O_{15}]^{3-}$.[2]

While the atomic connectivities for the anions of **1** and **2** are identical, there are significant differences in the metrical parameters, the most pronounced of which are the Mo(1)–Mo(2) bond lengths of 2.770(2) Å in **1** and 2.613(1) Å in **2** (Table IV). The bond distance observed for **2** lies within the normal range of Mo(V)–Mo(V) distances for binuclear units of this type and may be compared to the values of 2.60 Å (average) and 2.583 Å observed for other species exhibiting $\{Mo_2O_8\}$ units in close proximity to Na^+ cations. $[Na(H_2O)_3H_{15}Mo_{42}O_{109}\{(OCH_2)_3CCH_2OH\}_7]\cdot 15H_2O$[28] and $[Na\{Mo_6O_{15}(O_3PC_6H_5)(HO_3PC_6H_5)_3\}_2]^{9-}$,[29] respectively.

The relative elongation of the Mo(1)–Mo(2) bond distance of **1** is attributed to the structural influence of the Na^+ cation coordination geometry. As shown in Figure 2, the Na^+ coordination spheres of **2** are associated with doubly- and triply-bridging oxo-groups and the terminal O(9) of the $(HAs_3O_7)^-$ unit, while Na^+ cations of structure **1** are strongly associated with the $\{Mo{=}O\}$ terminal oxo groups of the binuclear units. The influence of the strongly electropositive Na^+ cations in **1** may serve to polarize the Mo(1)–O(2) and Mo(2)–O(5) bonds and concomitantly to reduce the electron density at the Mo centers and weaken the Mo–Mo bond interaction.

The different coordination geometries associated with the cations of **1** and **2** produce distinctly different structural networks as shown in Figure 2c,d. In the case of **2**, the cations are present as binuclear $\{Na_2(H_2O)_5\}^{2+}$ units, containing a single bridging aquo group and bridging pairs of $[Mo_4As_6O_{20}(OH)_2]^{4-}$ clusters

---

(24) Chen, Q.; Zubieta, J. *Coord. Chem. Rev.* **1992**, *114*, 104, and references therein.

(25) Stiefel, E. I. *Prog. Inorg. Chem.* **1977**, *22*, 1.

(26) Pope, M. T. *Prog. Inorg. Chem.* **1991**, *39*, 181.

(27) See, for example: Liu, S.; Shaikh, S. N.; Zubieta, J. *Inorg. Chem.* **1987**, *26*, 4305.

(28) Khan, M. I.; Zubieta, J. *J. Am. Chem. Soc.* **1992**, *114*, 10058.

(29) Cao, G.; Haushalter, R. C.; Strohmarier, K. G. *Inorg. Chem.* **1993**, *32*, 127.

Table IV. Comparison of Selected Bond Lengths (Å) and Angles (deg) for the Structures of 1 and 2

	1	2
Mo(1)–Mo(2)	2.770(2)	2.613(1)
Mo(1)–O(1)	2.127(10)	2.023(10)
Mo(1)–O(2)	1.702(11)	1.698(9)
Mo(1)–O(3)	1.892(11)	1.939(7)
Mo(1)–O(4)	1.992(11)	1.980(9)
Mo(1)–O(4a)	2.289(11)	2.299(8)
Mo(1)–O(7a)	2.058(11)	2.108(8)
Mo(2)–O(3)	2.064(11)	1.988(10)
Mo(2)–O(4)	1.904(11)	1.983(8)
Mo(2)–O(5)	1.712(12)	1.680(9)
Mo(2)–O(6)	2.022(12)	2.020(7)
Mo(2)–O(7)	2.282(10)	2.420(8)
Mo(2)–O(8)	2.111(12)	2.061(9)
As(1)–O(6)	1.799(12)	1.766(7)
As(1)–O(9)	1.700(14)	1.797(10)
As(1)–O(10)	1.869(11)	1.798(9)
As(2)–O(7)	1.788(11)	1.787(7)
As(2)–O(10)	1.745(12)	1.790(8)
AS(2)–O(11)	1.835(14)	1.791(10)
AS3-O(8)	1.670(14)	1.745(9)
AS(3)–O(11)	1.823(13)	1.816(8)
AS(3)–O(1a)	1.855(9)	1.758(8)
Na(1)–O(2)	2.473(12)	
Na(1)–O(3)		2.399(10)
Na(1)–O(4)		2.469(9)
Na(1)–O(5)	2.504(15)	
Na(1)–O(7)		2.493(11)
Na(1)–O(9)	2.627(13)	
Na(1)–O(10)	2.275(16)	
Na(1)–O(12)		2.364(12)
Na(1)–O(13)		2.352(11)
Na(1)–O(14)	2.444(17)	2.393(10)
Na(1)–O(16)	2.224(17)	
Na(2)–O(1)	2.217(15)	
Na(2)–O(3)	2.662(14)	
Na(2)–O(9)		2.638(12)
Na(2)–O(10)		2.419(11)
Na(2)–O(11)	2.379(16)	2.502(10)
Na(2)–O(12)	2.383(21), 2.662(18)	
Na(2)–O(14)		2.507(8)
Na(2)–O(15)	2.211(34)	2.350(13)
Na(2)–O(16)		2.309(15)
O(1)–Mo(1)–O(3)	153.4(4)	150.1(4)
O(2)–Mo(1)–O(4)	164.7(5)	167.3(3)
O(3)–Mo(1)–O(7)	160.6(4)	160.0(3)
O(3)–Mo(2)–O(8)	161.2(4)	156.4(3)
O(4)–MO(2)–O(6)	161.3(5)	155.0(3)
O(5)–MO(2)–O(7)	170.8(5)	172.0(4)

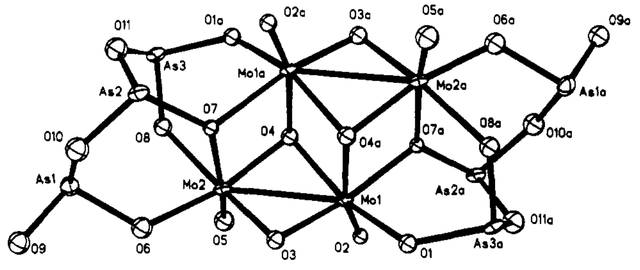

Figure 1. View of the molecular anion $[Mo_4As_6O_{20}(OH)_2]^{4-}$ of 1 and 2, showing the atom-labelling scheme.

to form infinite $[Na_2(H_2O)_5]_2[Mo_4As_6O_{20}(OH)_2]$ chains. In contrast, structure 1 exhibits two distinct binuclear cation sites, a doubly aquo-bridged $\{Na_2(H_2O)_6\}^{2+}$ unit and a singly bridged $\{Na_2(H_2O)_3\}^{+}$ site, which are located in the hydrophilic region between layers of $[Mo_4As_6O_{20}(OH)_2]^{4-}$ anions. The $\{Na_2(H_2O)_6\}^{2+}$ binuclear units interact with three anion sites, while the $\{Na_2(H_2O)_3\}^{+}$ unit associates with the {Mo═O} terminal oxo groups of one cluster and the pendant-OH group and the {As—O—As}-type oxo group of a cluster from an adjacent anion strand. The result is a complex three-dimensional network of anion strands interconnected by bridging cation units. While the N—O bond distances span a range of 2.21(3)–2.64(1) Å, such variations are not exceptional for Na^+ cations, and valence sum calculations suggest no discrepancies.[30]

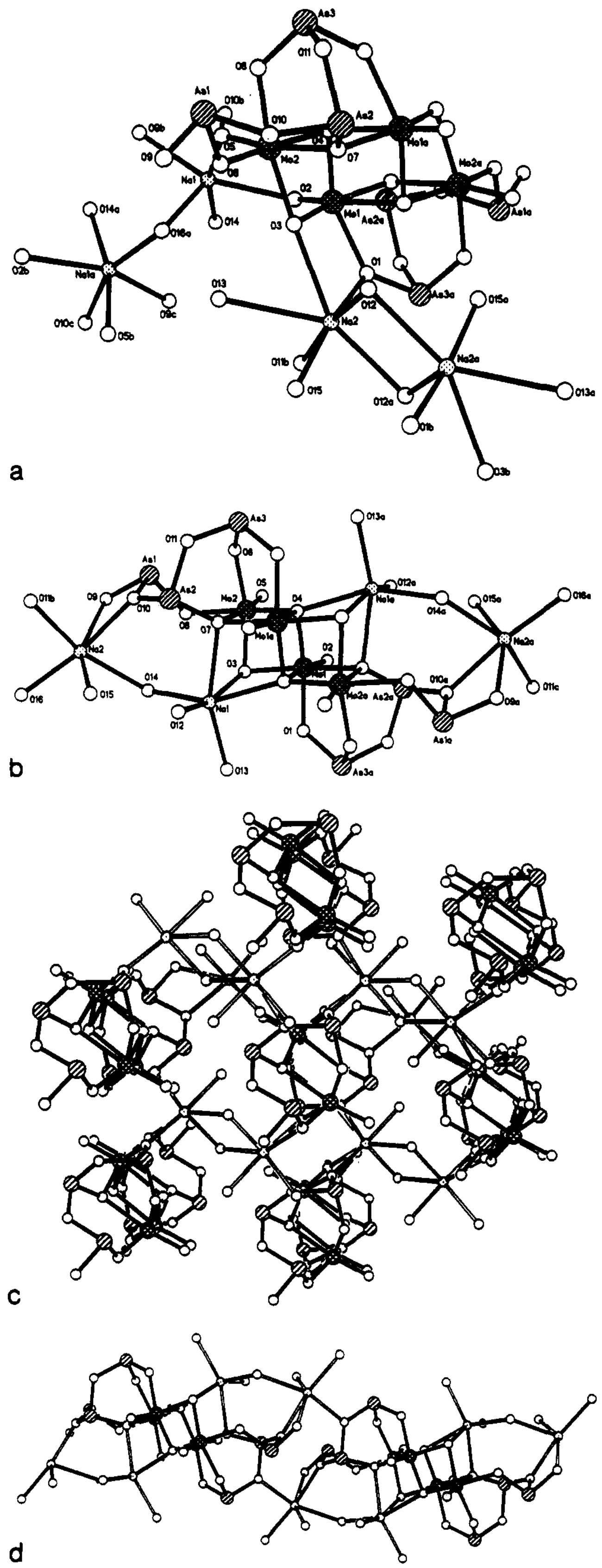

Figure 2. (a) Cation coordination about the $[Mo_4As_6O_{20}(OH)_2]^{4-}$ cluster in 1. (b) Cation coordination about the $[Mo_4As_6O_{20}(OH)_2]^{4-}$ cluster in 2. (c) Complex network of cation bridged anion clusters which results for 1. (d) Linear chains of associated cations and anions exhibited by the structure of 2.

The isolation of **1** and **2**, two distinct phases which are based on a common $[Mo_4As_6O_{20}(OH)_2]^{4-}$ cluster, demonstrates that relatively minor modifications in reaction conditions in hydrothermal preparations may result in unique structural types. Furthermore, while the templating influence of inorganic cations may be used to direct the synthesis of materials, the mechanism is not completely understood. Thus, the same template can lead to different structures or the same structure may be derived from different templates.[31] The preparations of **1** and **2** may reflect charge-compensation and space-filling effects of the template under modified reaction conditions.

Acknowledgment. This work was supported by NSF grant number CHE9119910.

Supplementary Material Available: Tables of experimental details, bond lengths and angles, and anisotropic temperature factors for **1** and **2**, respectively (14 pages). Ordering information is given on any current masthead page.

---

(30) Brown, I. D. In *Structure and Bonding in Crystals*; O'Keefe, M., Navrotsky, A., Eds.; Academic Press: New York; 1981; Vol. II, p 1.

(31) Stein, A.; Keller, S. W.; Mallouk, T. E. *Science* **1993**, *259*, 1558.